New data on Cs and Rb distribution between potassium feldspar and alkaline fluid: A study of th "trapping effect"

Article *in* Geochemistry International · August 2001

CITATION
1

READS
21

6 authors, including:

Vladimir Tauson
Russian Academy of Sciences
137 PUBLICATIONS **826** CITATIONS
SEE PROFILE

Vladlen Akimov
Institution of Geochemistry SB RAS
43 PUBLICATIONS **203** CITATIONS
SEE PROFILE

Joerg Goettlicher
Karlsruhe Institute of Technology
268 PUBLICATIONS **2,448** CITATIONS
SEE PROFILE

Alexander Rocholl
Helmholtz-Zentrum Potsdam - Deutsches GeoForschungsZentrum GFZ
74 PUBLICATIONS **3,116** CITATIONS
SEE PROFILE

Geochemistry International, Vol. 39, No. 8, 2001, pp. 725–731. Translated from Geokhimiya, No. 8, 2001, pp. 803–811.

New Data on Cs and Rb Distribution between Potassium Feldspar and Alkaline Fluid: A Study of the "Trapping Effect"

V. L. Tauson*, [1], V. K. Taroev*, V. V. Akimov*, J. Gottlicher, H. Pentinghaus**, and A. Rocholl*****

*Vinogradov Institute of Geochemistry, Siberian Division Russian Academy of Sciences, ul. Favorskogo 1a, Irkutsk, 664033 Russia

**Institute of Technical Chemistry, Water, and Geotechnology, Karlsruhe Research Center, D-76021 Karlsruhe, Germany

***Institute of Mineralogy, Heidelberg University, 69120 Heidelberg, Germany

[1]e-mail: vltauson@ige.irk.ru

Received March 12, 2000

Abstract—The effect of trapping a trace element, i.e., increasing element partitioning to the solid phase due to interaction of its atoms with crystal lattice defects, is an important phenomenon in trace-element behavior in geochemical systems. We have experimentally determined the coefficients of Rb and Cs cocrystallization with K in the K-feldspar–alkaline hydrothermal fluid system at 500°C and 1 kbar using highly sensitive methods with high-resolution for the analysis of solid phases (ICP-MS and ion microprobe). The fluid was sampled with a specially designed technique. Numerical modeling of Rb and Cs capture by K-feldspar crystal dislocation defects was based on real crystal structure data determined from X-ray powder diffraction measurements. Theoretical and experimental results show that, unlike Rb, Cs is accumulated in dislocation defects, and, at a low Cs content in K-feldspar, the Cs partition coefficient significantly increases. An inhomogeneous Cs distribution at a microscopic scale at a generally uniform Rb distribution and some earlier experimental data suggest that a significant amount of Cs in K-feldspar is confined to dislocations, and the trapping effect is important for this element at $<\sim 10^{-4}$ mol % $CsAlSi_3O_8$ in K-feldspar. This tendency to increasing co-crystallization coefficients is also observed at larger $CsAlSi_3O_8$ concentrations of >0.4 mol %. New special experiments are needed to estimate the errors caused by the nonisothermal sampling of fluid or using residual liquids for modeling of the high-temperature fluid composition. Such experiments should also demonstrate the applicability of the analytical methods used for studying solid phases with very low trace-element concentrations.

Rare alkalis are considered as ore components in granitoids and pegmatites and are important petrological indicators [1]. Rubidium is generally accumulated in potassium feldspar (*Kfs*). This mineral often has elevated Cs contents; however, high concentrations of this element are more typical of biotite. The systems including *Kfs* and hydrothermal fluid with Rb and Cs were studied experimentally in numerous papers [2–9].

The distribution of a rare alkali metal M between different solid phases is usually described by the reaction $K_{Kfs} + M_{fl} = M_{Kfs} + K_{fl}$. The constant of this reaction is considered as a partition coefficient of rare alkalis $D_M^{Kfs/fl} = \frac{M_{Kfs}}{K_{Kfs}} / \frac{M_{fl}}{K_{fl}}$ (or, more precisely, as a coefficient of M cocrystallization with K). The earlier data on this coefficient for 500°C are summarized in Table 1, because our study only referred to this temperature. Chelishchev used natural microcline [7, 8] or feldspar glass [7] as starting materials for the ion exchange experiments. Beswick [6] synthesized sanidines from gels and then used this starting material in the ion-exchange experiments with aqueous solutions of (Rb,K)Cl. Eugster [2, 3] and Volfinger [9] applied the method of mineral synthesis in the $(K,Cs)AlSi_3O_8$–H_2O and K_2O–Al_2O_3–SiO_2–KCl–MCl–H_2O systems, respectively. An analysis of Table 1 shows that the data obtained for Rb are generally consistent, and *D* varies from 0.17 to 0.42. However, there are two discrepant groups of data for Cs (Volfinger versus Eugster and Chelishchev). The disagreement is also prominent in the temperature dependence of the partition coefficient: it is almost independent of temperature in [9] and significantly depends on this parameter in [2, 3, 7, 8]. All these data correspond to 1 kbar. However, Eugster demonstrated that pressure (1–2 kbar) does not affect the $D_{Cs}^{Kfs/fl}$ value [3]. These inconsistencies could be partially accounted for by differences in the fluid composition and the state of the starting material, including various degrees of *Kfs* ordering. However, data in [5, 8] allow us to conclude that the specified factors could not cause such a strong divergence and that some other effects should be taken into account. Very low Rb and Cs contents in *Kfs* (from 10^{-4} mol % of corresponding end-members) were used only by Volfinger, who applied a radioisotopic method for determining rare alkalis both in fluid (residual liquid) and solid phases.

Table 1. Available data on Rb and Cs distribution between potassium feldspar and fluid phase at 500°C

Reference	System	Element	$D_M^{Kfs/fl}$	Interval of M concentrations in *Kfs*, mol %	Method of M determination
[3]	Sanidine (synt.) + H_2O	Cs	0.48	2×10^{-2}–1	Radioisotopic (RI)
[7]	Glass + alkaline solution or natural microcline + alkaline solution	Cs	0.46*	≤5	Flame photometry (FP)
		Rb	0.42*	≤5	
[8]	Sanidine (synt.?) + alkaline solution	Cs	0.46**	?	FP
		Rb	0.41**	?	
	Natural microcline + alkaline solution	Cs	0.43**	1.2–12	
		Rb	0.36**	0.9–7	
[6]	Sanidine (synt.) + (Rb, K)Cl + H_2O	Rb	0.17 ± 0.04	0.8–7	FP
[9]	$K_2O + Al_2O_3 + SiO_2 + KCl + MCl + H_2O$	Cs	0.023 ± 0.03	1.3×10^{-4}–0.16***	
		Rb	0.408 ± 0.10	6.6×10^{-4}–18.7	RI

* Data are taken from diagrams.

** Data are taken from Table 14 in [8]. Data in Fig. 26 from [8] contradict this table and are probably erroneous.

*** The points with high Cs contents of 1.7 and 21.8 mol % of the Cs end-member are excluded; 0.142 and 0.5 are respective $D_{Cs}^{Kfs/fl}$ values.

Eugster also used this method, but obtained different results for the Cs end-member contents ranging from 10^{-2} to 1 mol % (Table 1). This interval was also studied in [9]. Thus, the observed discrepancy probably is not caused by differences in analytical methods or the concentrational dependence $D_{Cs}^{Kfs/fl}$, which may be related to the deviation of the solid solution from ideality at >1 mol % Cs end-member [10, 11].

An analysis of the information presented in the publications cited above reveals some other important factors that could affect the results. First, all the researchers used residual liquids to describe the characteristics of a high-temperature fluid. This approach would not be appropriate if unmixing phenomena were assumed in alkaline silicate solutions [12]. Second, low Rb and Cs concentrations in *Kfs* have not been determined directly, whereas radioisotopic measurements only give the bulk concentration of a radioisotope in the experimental solid phases including quench phases or phases crystallized on cooling of a heterogeneous silicate-rich heavy liquid. Third, the authors did not analyze the real structures of the *Kfs* crystals.

However, the modeling results demonstrate that the trapping phenomena could be observed in systems with Cs, i.e., at increasing element partitioning to the solid phase at very low concentrations of elements dissolved in *Kfs* due to the interaction of ions with crystal lattice defects [13]. The effect of increasing Cs concentrations in imperfect orthoclase crystals was analyzed within the model of the symmetrical tilt boundary [14], and the results were compared with experimental data. Unfortunately, primary experimental information [10] was not available to the authors of [13, 14], and they used Mysen's data [15], which were found later to be incorrect. Actually, the original data are identical to those obtained by Volfinger [9] and show $D_{Cs}^{Kfs/fl}$ to increase at high Cs contents, rather than at low concentrations of this element. Thus, inconsistency exists between the data obtained by different researchers, and it is not clear whether the trapping effect occurs in the system considered or not. Therefore, the previous papers cannot serve as an appropriate basis for the solution of this problem. We performed a new study of Rb and Cs distribution between *Kfs* and alkaline fluid. This study differs in that the fluid composition is determined by direct sampling, the real structure of *Kfs* crystals is taken into account, and Rb and Cs are analyzed with modern analytical techniques in individual crystals or small monomineral separates.

EXPERIMENTAL PROCEDURE

The distribution of alkali metals between solid and fluid phases was studied by synthesizing *Kfs* from starting mixtures of Al and Si oxides in aqueous KOH solutions with added RbOH and CsCl. Reagents were analytically pure Al_2O_3 and SiO_2, pure KOH and RbOH, and ultrapure CsCl. Although the KOH reagent used in our experiments contained the lowest Rb ($<10^{-3}$ wt %) among the other available potassium reagents, we failed to reach the very low Rb contents in the system.

The experiments were performed in stainless steel autoclaves with copper reaction containers (liners) of about 80 cm^3 in volume. The containers were sealed using argon-shielded arc welding. A copper sampler was fixed to the liner lid with a pin junction. The sampler is designed to collect enough of the high-temperature fluid for analysis. The analogous reaction container was used in our previous experiments on Pb distribution between *Kfs* and fluid (see figure in [16]). Experi-

ments lasted 40 days at 500°C and 1 kbar (100 MPa). The autoclaves were quenched in cold water.

ANALYTICAL TECHNIQUE

The solutions were analyzed by flame photometry (FP) and atomic absorption spectrometry (AAS). Solid phases were studied optically and by X-ray powder diffraction (XRD). They were analyzed for K, Rb, and Cs using FP, ICP-MS, and an ion microprobe. The FP measurements were performed using a flame photometer based on DFS-12. The photometer was calibrated by standard K, Rb, and Cs solutions. The detection limit was 3 ppm and the error was ±10% for the rare alkali metals.

The AAS measurements were performed using a Perkin–Elmer 503 unit with Rb and Cs detection limits of 1 ppb and errors within ±5%. A PQ-2 VG Instruments Quadrupole mass-spectrometer at the Institute of Limnology, Siberian Division, Russian Academy of Sciences, was used for ICP-MS determination. The analysis of small concentrations was performed in a counting mode, while high concentrations were analyzed in an analog mode. Determination errors were within ±5%. BHVO-1, BCR-1, and AGV-1 were used as standards.

The solid phases were analyzed also by a Cameca IMS-3f ion microprobe at the Mineralogical Institute of Heidelberg University. Polished samples were coated with a gold film, and secondary ions were generated by bombardment of the sample with a 20-nA $^{16}O^-$ primary beam. A primary acceleration voltage of 12.5 kV was applied, the beam diameter was 50 μm, the image field was 25 μm, the high deflecting voltage was –60V, and the energy window was 30 eV. Preparatory to analyses, the primary beam was equilibrated for 10 min. ^{85}Rb and ^{133}Cs were measured for 2 and 3 s, respectively, and normalized to ^{30}Si (1 s). Data were collected from 15 blocks of 3 cycles each, with the total analysis time of 13 min. Depending of the size of crystals, 1 to 3 analyses were obtained from each, with 2–3 crystals from each experiment used. The measured intensities were recalculated to element concentrations using a NIST SRM 612 standard [17].

The average effective dimensions of crystallites (i.e., the thickness of coherent scattering domains or blocks) and values of lattice strain of the *Kfs* crystal structure were calculated from the line profiles of $(\bar{2}01)$, (060), and $(\bar{2}04)$ reflections in the X-ray diffraction powder pattern. A natural microcline was used as a standard to account for the instrumental broadening of line widths. This microcline sample showed the smallest broadening of diffraction line widths among many samples studied. Measurements were performed with a powder diffractometer DRON-3 using CuK_α radiation. Calculations were made with the harmonic analysis of the reflection profile [18]. The dimensions obtained for crystal domains (D) and mean square values of relative microdistortions ($\sqrt{\langle\varepsilon\rangle^2}$) were used for revealing the characteristics of a dislocation ensemble (dislocation densities, ρ, and dislocation spacing, d) within the model developed by Krivoglaz [19].

EXPERIMENTAL RESULTS

Potassium feldspar and kalsilite in various proportions were synthesized in the experiments. The *Kfs* crystals were up to 1–2 mm long. Their habits [20] were different from kalsilite crystals and were sufficiently separated for analysis. *Kfs* had an Al/Si ordering parameter $2t_1$ of about 0.6, which corresponds to sanidine crystallization under conditions of forced equilibrium [21, 22]. The following values characterizing the *Kfs* crystal structure were determined: D = 28–39 nm, $\sqrt{\langle\varepsilon\rangle^2} = 4.5–8.0 \times 10^{-3}$, $\rho = 3–7 \times 10^{-10}$ cm^{-2}.

In contrast to Al/Si ordering, the equilibrium of alkali metals ion exchange with *Kfs* is usually rapidly achieved in experiments. We believe that, in the synthesis method applied, the isothermal growth of crystals provides the equilibrium distribution of microcomponents; i.e., their atoms can easily occupy physical fields of growth dislocations and dislocation pile-ups, because of high rates of alkali element exchange at the crystal/fluid boundary. Kalsilite (*Kls*) formation can change the composition of the fluid from which *Kfs* crystallized. However, we believe that it cannot affect the coefficient of M cocrystallization with K in *Kfs* for the following reasons: (1) *Kfs* is dominant in most experiments (Table 2), and (2) the equality of chemical potentials of M and K in *Kls*, *Kfs*, and fluid is met simultaneously; i.e., $\mu_M^{Kfs} = \mu_M^{fl}$, $\mu_K^{Kfs} = \mu_K^{fl}$ and $\mu_M^{Kls} = \mu_M^{fl}$, $\mu_K^{Kls} = \mu_K^{fl}$. The kalsilite crystallization can only change the element concentration and M/K ratio in fluid. This may result in a new M/K ratio in *Kfs* to meet the exchange reaction constant.

Table 2 shows the *Kfs* compositions determined by various methods. The element contents measured by ICP-MS and ion microprobe normally differ by not more than ±20%, and this deviation is more significant only at very low Cs contents (<~10^{-4} wt %). The ion microprobe data were preferred in the latter case, because by using this technique we could control the phase and chemical homogeneity of *Kfs* crystals. A crystal synthesized in run 5 (Table 2) was analyzed by ion microprobe. The Cs concentrations determined in successive cycles of ion microprobe measurements differ by about one order of magnitude. Rubidium was rather homogeneously distributed in this crystal. Unfortunately, we could not study concentrations of the Rb end-member below 7×10^{-3} mol % in *Kfs*, because the initial KOH contained about ~10^{-3} wt % Rb. Cesium has not been detected by ICP-MS in the initial KOH. However, the data obtained in run 8 (Table 2) may indicate the collective influence of various sources (includ-

Table 2. Experimental results on Rb and Cs distribution between *Kfs* and alkaline hydrothermal fluid at 500°C and 1 kbar

Run	Composition of initial solution in wt %			Synthesized phases	Composition of solution in sampler					Composition of *Kfs* crystals				$D_M^{Kfs/fl}$	
					ppm			at. ratio		ppm		at. ratio			
	KOH	RbOH	CsCl		K	Rb	Cs	Rb/K	Cs/K	Rb	Cs	Rb/K	Cs/K	Rb	Cs
1	11.60	0.89	1.10	*Kfs* > *Kls*	10740	709	262	3.0×10^{-2}	7.2×10^{-3}	10600	12490	3.7×10^{-2}	2.8×10^{-2}	1.2	3.9
2	11.60	0.89	1.10	*Kls* > *Kfs*	15730	177	65	5.1×10^{-3}	1.2×10^{-3}	1540	1900	5.0×10^{-3}	4.0×10^{-3}	1.0	3.3
3	13.80	0.13	0.14	*Kfs* > *Kls*	6390	110	9.0	7.9×10^{-3}	4.1×10^{-4}	1300	540	4.2×10^{-3}	1.1×10^{-3}	0.5	2.7
4	13.00	0.03	0.02	*Kfs* > *Kls*	8600	10.2	2.2	5.4×10^{-4}	7.5×10^{-5}	225	28	7.3×10^{-4}	5.9×10^{-5}	1.4	0.8
5	13.00	0.03	0.02	*Kls* > *Kfs*	9800	2.0	0.1	9.3×10^{-5}	3.0×10^{-6}	30	2.8	9.8×10^{-5}	5.9×10^{-6}	1.1	2.0
6	15.25	0.0003*	10^{-4}	*Kfs* > *Kls*	24600	6.0	0.01	1.1×10^{-4}	1.2×10^{-7}	32	0.4	1.0×10^{-4}	8.4×10^{-7}	0.9	7.0
7	15.25	0.0002*	10^{-5}	*Kfs* = *Kls*	20400	2.9	0.01	6.5×10^{-5}	1.4×10^{-7}	28	0.3	9.1×10^{-5}	6.3×10^{-7}	1.4	4.5
8	15.25	0.01	–	*Kfs* > *Kls*	16800	4.2	0.002	1.1×10^{-4}	3.5×10^{-8}	41	0.05**	1.3×10^{-4}	1.6×10^{-7}	1.2	4.6
9	15.25	0.0002*	0.01	*Kfs* > *Kls*	13140	2.0	0.03	7.0×10^{-5}	6.7×10^{-7}	22	0.7	7.2×10^{-5}	1.5×10^{-6}	1.0	2.2

* Including about 0.0002% Rb from the KOH reagent containing ~10^{-3}% Rb.

** Supposedly from initial reagents and material of copper container.

The K proportion was calculated from stoichiometric (K, Rb, Cs)$AlSi_3O_8$. The SiO_2/Al_2O_3 mol ratio was preset at 10.2 in all runs except for runs 2 and 5, where the SiO_2/Al_2O_3 ratio equaled 11.1. Methods of *Kfs* analysis: runs 2 and 9—ion microprobe: 4, 6–8 (Cs)—ICP-MS; 1, 5, 8 (Rb)—ion microprobe and ICP-MS (averaged data); 3—AAS. Abbreviations: *Kfs*—potassium feldspar, *Kls*—kalsilite, M = Rb or Cs.

ing the copper container), each of which has Cs concentrations below the detection limit. Dependences of partition coefficients on crystal compositions (in mol % $MAlSi_3O_8$) are shown in Fig. 1. $D_{Rb}^{Kfs/fl}$ is almost constant within the interval studied of the crystal compositions and is equal to about one. Cesium distribution is more complex. The coefficient of its cocrystallization with K increases both at low (<10^{-4} mol %) and high (>10^{-1} mol %) $CsAlSi_3O_8$ contents in *Kfs*.

NUMERICAL MODELING RESULTS

The modeling is based on the formalism developed by Abramovich *et al.* [23, 24] and is considered in detail in [14]. The model adopted suggests the dominating role of inhomogeneous elastic fields of dislocation pile-ups forming the subgrain boundaries in the distribution of impurities in *Kfs* crystals. In contrast to the classical trapping effect [25] caused by the interaction of impurities with thermal defects, whose concentrations increase with increasing temperature, the effect considered can occur at medium and low temperatures and decreases with increasing temperature. Our calculation is based on the model of the symmetrical tilt boundary. All the necessary calculation parameters were taken from the publication used in [14]. The calculations were performed for D = 40 nm and d = 10 nm corresponding to dislocation densities and block dimensions observed in the synthesized *Kfs* crystals.

The numerical modeling results are shown in Fig. 2. Rubidium is not accumulated by dislocation defects, generally due to the small volume effect of Rb for K substitution. By contrast, Cs is significantly accumulated and its bulk concentration in the imperfect crystals (x_{bulk}) can exceed the equilibrium concentration within the undistorted domains (x_0) by more than one order of magnitude. If the amount of element in the system is high enough ($m_{Cs}^{fl} > m_{Cs}^{cr}$, in our case), the coefficient of Cs distribution between *Kfs* and fluid also increases proportionally. Different Cs behavior at various element contents in Fig. 2 is related to specific features of the adopted model. At very low concentrations (<~10^{-5} mol %) both the distorted crystal layers next to the dislocation boundaries and the undistorted layers can be considered as diluted solid solutions. In this case, according to the main equation of the effect [14, 23, 24], the x_{bulk}/x_0 ratio depends only on the linear (relative to ln x) terms and has a constant value determined only by the strain induced by the corresponding structural

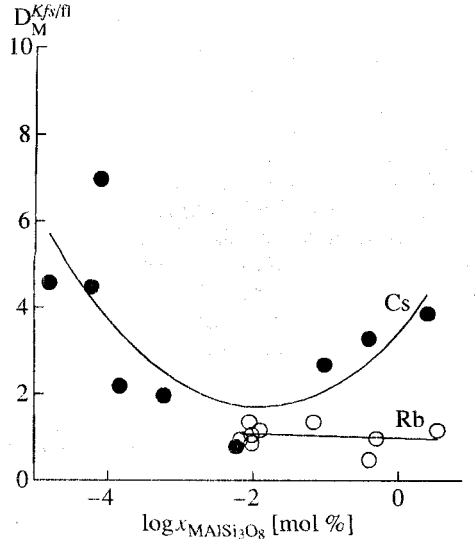

Fig. 1. Coefficients of Cs and Rb partitioning between *Kfs* and alkaline fluid versus concentration of elements in the synthesized crystals (500°C, 1 kbar).

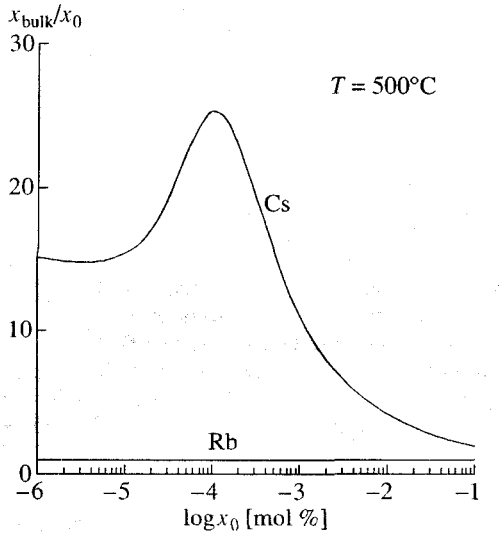

Fig. 2. Numerical modeling results for the effect of Rb and Cs accumulation in the imperfect orthoclase crystals. Model of symmetrical tilt boundary. Dislocation spacing is 10 nm, domain size is 40 nm (4 dislocations in each dislocation wall). x_{bulk} is the bulk concentration of impurity in an imperfect crystal, x_0 is the equilibrium concentration in undistorted crystal slices (mol % of corresponding end-member).

imperfection. At x_0 between ~10^{-5} and ~10^{-4} mol % (Fig. 2), the x_{bulk}/x_0 ratio increases, because the x_{bulk} value within this interval is contributed not only by linear (relative to ln$x$) terms, but also by higher power terms. Such behavior is typical of impurities that can be effectively entrapped by structural defects in a crystal. Finally, at $x_0 > 10^{-4}$ mol %, the constraint on the local concentration takes an important value: this concentration should not exceed the value corresponding to the chemical spinodal (the model suggests that states between the binodal and spinodal can exist as metastable and only the states below the chemical spinodal are absolutely unstable [14]). As a result, the x_{bulk}/x_0 ratio does not increase further and a maximum occurs at 10^{-4} mol % (Fig. 2), because the distorted layers in the crystal structure are saturated with impurity atoms and the x_{bulk} becomes constant, while x_0 continues to grow. The x_{bulk}/x_0 ratio consequently decreases and approaches unity at $x_0 \longrightarrow x_{spin}$ (x_{spin} corresponds to the composition of chemical spinodal at a given temperature).

DISCUSSION

The following two aspects are emphasized in the discussion: (1) a comparison of the obtained distribution coefficients with experimental data (Table 1), and (2) an estimation of the probability for the effect of alkali metals trapping by dislocation defects in the *Kfs* crystals. As we mentioned in the introduction, there are significant inconsistencies in the results of previous studies of Cs behavior. Our data show larger partition coefficients for both alkali metals, particularly for Cs (Table 2, Fig. 1). Let us recall, however, that all the researchers analyzed the residual liquids and significant errors could have been introduced, particularly in the case of fluid immiscibility [12]. Moreover, the very small Rb and Cs concentrations have not been measured directly in the investigations cited. This may result in errors related to an underestimation of quench phases and sorbed element forms, even if the liquid immiscibility did not occur in experiments. However, our data also cannot be preferred, because the method of nonisothermal sampling allows errors due to possible unequal conditions of autoclave cooling and changes in fluid composition on cooling from the run temperature (500°C) to the critical temperature of a solution with a given composition (~380°C). Difficulties of isothermal and isobaric sampling in the silicate systems are well known. We would recommend using our sampling technique under conditions close to the critical temperature. In this case, more reliable cocrystallization coefficients can be obtained, and possible errors related to the nonisothermal sampling and analysis of residual liquids can be estimated.

According to the semi-empirical model of Blundy and Wood [26] that is based on the differences between ionic radii, the cesium partition coefficient should be one–two orders of magnitude lower than that of rubidium (see also [27]). The fact that $D_{Cs}^{Kfs/fl}$ is approximately of the same order of magnitude as $D_{Rb}^{Kfs/fl}$ (Table 1)

or even larger (according to our data) could indicate the occurrence of the trapping effect. As we mentioned above, the ion microprobe detects inhomogeneities in Cs distribution in *Kfs* crystals at concentrations of several ppm and lower. This may reflect the inhomogeneous distribution of dislocation defects during the crystal growth and the occurrence of both isomorphic cesium and cesium confined to dislocations. Note that the inhomogeneous Cs distribution is probably not related to the chemical instability of crystal growth, because rubidium, the other impurity element, is homogeneously distributed, and the Al/Si ordering parameter of the synthesized crystals corresponds to stationary growth and to conditions of forced equilibrium [14, 22].

The higher dispersion of Cs in comparison to Rb in alkali feldspars of various origins is also revealed in some other studies. This phenomenon could be related to the conditions of the growth or postgrowth transformation of crystals and to the active entrapment of incompatible (in terms of ionic radii) elements by defects [28]. Although no direct and definite evidence for the occurrence of a dislocation-confined form of Cs in *Kfs* has yet been obtained, the factors discussed above and the numerical simulation results (Fig. 2) prove the influence of this effect on the Cs partition coefficient. Moreover, Akimov and Parkhomenko [29] used thermal atomic absorption to identify Cs forms in mechanically activated *Kfs* and concluded that a new Cs form with a lower release temperature (than the isomorphic impurity) appears in *Kfs*. This form is probably related to the interaction of Cs atoms with structural defects (particularly, with dislocation defects). Actually, the numerical estimates (Fig. 2) indicate significant Cs accumulation in imperfect orthoclase crystals with $<10^{-3}$ mol % $CsAlSi_3O_8$. A distinct increase of $D_{Cs}^{Kfs/fl}$ is detected in our experiments at $<10^{-4}$ mol % $CsAlSi_3O_8$, and this effect is notably less than could be expected from the theory. The discrepancy could be related to the inadequacy of the dislocation structure model of *Kfs* crystals (a more precise study of this structure requires the employment of electron microscopy) and to errors in the parameter values used (elastic moduli and interaction parameters). However, $D_{Cs}^{Kfs/fl}$ also tends to increase at higher Cs contents >0.4 mol % (Fig. 1). This increase was explained by the nonideality of K and Cs mixing in the solid solution [10, 11]. However, we also cannot exclude the influence of the Cs state in solution and the experimental errors mentioned above. In general, the concentrational dependence of partition coefficients at high impurity contents is not unusual during crystallization [30]. One of the possible reasons of this phenomenon is the formation of a fine dissemination of Cs microphases (for example, pollucite $CsAlSi_2O_6$), which have not yet been detected during phase analysis. These phases were not found by the ion microprobe, but its resolution could be insufficient to recognize the ultrafine phases. The occurrence of such phases could also increase the $D_{Cs}^{Kfs/fl}$ value in comparison to the value related to the isomorphic impurity.

CONCLUSION

A series of experimental data, i.e., the increase of $D_{Cs}^{Kfs/fl}$ at low Cs contents, the inhomogeneous distribution of this element, and the occurrence of a new Cs form in crystals with high dislocation densities [29], as well as theoretical analysis, indicate the important role of the trapping effect in Cs distribution between *Kfs* and hydrothermal fluid. However, some details are not clear yet and require additional studies including electron microscopy. The experimental data also demonstrate that the trapping effect does not occur for Rb, which is generally consistent with the theoretically predicted behavior of this element [13, 14].

Note that in addition to the structural defects discussed in this paper, the impurities can be also entrapped by twin planes. For example, defect clusters, impurity accumulation, and changes in the ordering of cation distribution between tetrahedral and octahedral sites in synthetic gem spinel are confined to twin planes [31, 32]. Pentinghaus [33] discussed similar phenomena in *Kfs* and suggested that the Carlsbad B twin plane could be responsible for nonstoichiometric defects. The influence of such defects on the entrapment of impurity elements is an interesting topic for further study.

ACKNOWLEDGMENTS

We thank G.P. Sandimirova (Institute of Geochemistry, Siberian Division, Russian Academy of Sciences) for her help in the atomic absorption and ICP-MS analyses. We are grateful to Professor R. Altherr (Mineralogical Institute, Heidelberg University) for allowing the ion microprobe analysis. The study was supported by the Russian Foundation for Basic Research, project no. 96-05-00054G, and the German Scientific Foundation, project no. 436 RUS 113/388/0 (R).

REFERENCES

1. Stavrov, O.D., Principal Geochemical Properties of Lithium, Rubidium, and Cesium at the Formation of Granite Intrusions and Related Pegmatites, in *Geologiya mestorozhdenii redkikh elementov* (Geology of Rare-Element Deposits), Moscow: Gosgeoltekhizdat, 1963, issue 21.
2. Eugster, H.P., Distribution Coefficients of Trace Elements, *Carnegie Inst. Washington*, 1954, Year Book 53, pp. 102–104.
3. Eugster, H.P., The Cesium–Potassium Equilibrium in the System Sanidine–Water, *Carnegie Inst. Washington*, 1955, Year Book 54, pp. 112–114.
4. Lagache, M., Etude experimentale de la repartition du cesium entre les feldspaths sodi–potassiques et des solutions hydrothermales à 700°C, 1 kbar, *Compt. Rend. Acad. Sci. Paris*, 1971, vol. 272, pp. 1328–1330.

5. Lagache, M. and Sabatier, G., Distribution des elements Na, K, Rb et Cs à l'état de trace entre feldspaths alcalins et solutions hydrothermales à 650°C, 1 kbar: Données experimentales et interpretation thermodynamique, *Geochim. Cosmochim. Acta*, 1973, vol. 37, no. 12, pp. 2617–2640.
6. Beswick, A.E., An Experimental Study of Alkali Metal Distributions in Feldspars and Micas, *Geochim. Cosmochim. Acta*, 1973, vol. 37, no. 2, pp. 183–208.
7. Chelishchev, N.F., Partitioning of Trace Amounts of Rare Alkali Metals between Potash Minerals of Granites and Aqueous Solutions: Evidence from Experimental Studies under Elevated Temperatures and Pressures, *Dokl. Akad. Nauk SSSR*, 1967, vol. 175, no. 5, pp. 1140–1142.
8. Chelishchev, N.F., *Ionoobmennye svoistva mineralov* (Ion-Exchange Properties of Minerals), Moscow: Nauka, 1973.
9. Volfinger, M., Effect de la temperature sur les distributions de Na, Rb et Cs entre la sanidine, la muscovite, la phlogopite et une solution hydrothermale sous une pression de 1 kbar, *Geochim. Cosmochim. Acta*, 1976, vol. 40, no. 3, pp. 267–282.
10. Roux, J., Volfinger, M., Lagache, M., *et al.*, Ideal Solid Solution Formation by Substitution of Alkali Earth Elements in Silicates, *Mineral. Soc. Jpn. Spec. Pap.*, 1971, vol. 1, pp. 214–221.
11. Iiyama, J.T. and Volfinger, M., A Model for Trace-Element Distribution in Silicate Structures, *Mineral. Mag.*, 1976, vol. 40, no. 314, pp. 555–564.
12. Rumyantsev, V.N., Immiscibility in Alkali Silicate Solutions under Elevated Pressures and Temperatures: On the Problem of the Structure of Hydrothermal Quartz-Generating Systems, *Zap. Vseross. Mineral. O–va.*, 1999, no. 1, pp. 125–130.
13. Urusov, V.S. and Dudnikova, V.B., A Mechanism for an Increase in the Distribution Coefficient of Trace Components during Crystallization: The Trapping Effect. Isovalent Systems, *Geokhimiya*, 1993, no. 4, pp. 499–514.
14. Urusov, V.S., Tauson, V.L., and Akimov, V.V., *Geokhimiya tverdogo tela* (Geochemistry of Solids), Moscow: GEOS, 1997.
15. Mysen, B.O., Limits of Solution of Trace Elements in Minerals According to Henry's Law: Review of Experimental Data, *Geochim. Cosmochim. Acta*, 1978, vol. 42, no. 6, pp. 871–885.
16. Taroev, V.K., Tauson, V.L., Suvorova, L.F., *et al.*, Lead Partition between Potash Feldspar and Alkaline Fluid in the SiO_2–Al_2O_3–PbO_2–KOH–H_2O System at 500°C and 100 MPa, *Dokl. Akad. Nauk*, 1997, vol. 356, no. 6, pp. 815–817.
17. Pearce, N.J.G., Perkins, W.T., Westgate, J.A., *et al.*, A Compilation of New and Published Major and Trace Element Data for NIST SRM 610 and NIST SRM 612, *Geostand. Newsl.*, 1997, vol. 21, no. 1, pp. 115–144.
18. Tauson, V.L. and Abramovich, M.G., *Fiziko-khimicheskie prevrashcheniya real'nykh kristallov v mineral'nykh sistemakh* (Physicochemical Transformations of Real Crystals in Mineral Systems), Novosibirsk: Nauka, 1988.
19. Krivoglaz, M.A., *Teoriya rasseyaniya rentgenovskikh luchei i teplovykh neitronov real'nymi kristallami* (Theory of the Scattering of X-rays and Slow Neutrons by Real Crystals), Moscow: Nauka, 1967.
20. Taroev, V.K., Tauson, V.L., and Abramovich, M.G., On the Problem of the Initial State of Ordering in Potash Feldspar Crystals: Experimental Results, *Geokhimiya*, 1991, no. 3, pp. 434–437.
21. Taroev, V.K. and Tauson, V.L., Crystallization Disordering of Potash Feldspar and Its Geochemical Significance, *Geol. Geofiz.*, 1991, no. 6, pp. 68–75.
22. Tauson, V.L. and Akimov, V.V., Introduction to the Theory of Forced Equilibria: General Principles, Basic Concepts, and Definitions, *Geochim. Cosmochim. Acta*, 1997, vol. 61, no. 23, pp. 4935–4943.
23. Abramovich, M.G., Tauson, V.L., and Akimov, V.V., Concentration of Trace Components in Structurally Imperfect Mineral Crystals, *Dokl. Akad. Nauk SSSR* 1989, vol. 309, no. 2, pp. 438–442.
24. Abramovich, M.G., Shmakin, B.M., Tauson, V.L., and Akimov, V.V., Indicator Chemical Characteristics of Minerals: Abnormal Contents of Trace Components in Structurally Imperfect Solid Solutions, *Zap. Vses. Mineral. O–va.*, 1990, vol. 119, no. 1, pp. 13–22.
25. Urusov, V.S. and Kravchuk, I.F., Trace Component Entrapment by Crystal Defects and Its Geochemical Significance, *Geokhimiya*, 1978, no. 7, pp. 963–978.
26. Blundy, J. and Wood, B., Prediction of Crystal–Melt Partition Coefficients from Elastic Module, *Nature* (London), 1994, vol. 372, pp. 452–454.
27. Urusov, V.S., *Teoriya izomorfnoii smesimosti* (The Theory of Isomorphism), Moscow: Nauka, 1977.
28. Ahrens, L.H., Notes on the Rb–Cs Dispersion Relationship, with Particular Reference to Pegmatite Microclines from the Sayan Mountains, USSR, *Geochim. Cosmochim. Acta*, 1966, vol. 30, no. 1, pp. 105–107.
29. Akimov, V.V. and Parkhomenko, I.Yu., Natural Structure and Absorptive Properties of Mechanically Activated Feldspars, *Tezisy dokladov III Mezhdunarodnoi konferentsii "Kristally: rost, svoistva, real'naya struktura, primenenie"* (Abstracts of Pap. III Int. Conf. Crystals: Growth, Properties, Natural Structure, and Use), Aleksandrov: VNIISIMS, 1997, pp. 145–147.
30. Barthel, J., Buhrig, E., Hein, K., *et al.*, *Kristallisation aus Schmelzen*, Leipzig: Deutscher Verlag für Grundstoffindustrie, 1983. Translated under the title *Kristallizatsiya iz rasplavov. Spravochnik*, Moscow: Metallurgiya, 1987.
31. Carter, C.D., Elgat, Z., and Shaw, T.M., Twin Boundaries Parallel to the Common {111} Plane in Spinel, *Philos. Mag.*, 1987, vol. 55, no. 1, pp. 1–19.
32. Carter, C.D., Elgat, Z., and Shaw, T.M., Lateral Twin Boundaries in Spinel, *Philos. Mag.*, 1987, vol. 55, no. 1, pp. 21–38.
33. Pentinghaus, H.J., Polymorphie in den feldspatbildenden Systemen A + T3 + T34 + O8 und A2 + T23 + T24 + O8 Alkali- und Erdalkali-, Bor-, Aluminium-, Gallium-, Eisen-Silikate und Germanate, *Habilitationsschrift im Fachbereich Chemie der Westfalischen Wilhelms-Universitat*, Munster, 1981.